THE JOURNAL OF PHYSICAL CHEMISTRY B

Article

pubs.acs.org/JPCB

Precipitate Deposition around CMC and Vesicle-to-Micelle Transition of Monopotassium Monododecyl Phosphate in Water

Takaya Sakai,*[,†] Masahiro Miyaki,[‡] Hitoshi Tajima,[‡] and Masaki Shimizu[§]

[†]Research and Development - Eco-Innovation Research, Kao Corporation, 1334 Minato, Wakayama-shi, Wakayama 640-8580, Japan

[‡]Research and Development - Beauty Research, Kao Corporation, 2-1-3 Bunka, Sumida-ku, Tokyo 131-8501, Japan

[§]Product Development Research Laboratories, Kao (China) Research and Development Center Co. Ltd., 623 Zi Ri Road, Minghang District, Shanghai 200241, P. R. China

ABSTRACT: Monoalkyl phosphate (MAP) salts are a kind of bivalent anionic surfactants. The difference of properties between half-neutralized monosalt and completely neutralized disalt is very interesting. In this study, the aggregation behavior of monopotassium monododecyl phosphate (MAP-12K) in aqueous solution with an increase in concentration was investigated by surface tension (γ), elemental analysis, gas chromatography, differential scanning calorimetry, steady-state fluorescence, and negative strained transmission electron microscopy techniques. MAP-12K aqueous solution showed some characteristics: (I) Vesicle aggregates were formed at very dilute concentration (1.2 mM). (II) The precipitate of a highly hydrophobic dimer of MAP, which was quaternary neutralized by potassium, was generated only in a certain dilute concentration region (2.7−200 mM) around the critical micelle concentration (cmc = 20 mM). (III) Vesicles spontaneously translate into micelles at the cmc. (IV) In the higher concentration above 200 mM, the solution becomes homogeneous micellar solution. All of these uncommon characteristics are thought to be caused by the generation of the dimer, which is much more hydrophobic than dissolved MAP derivatives, in the complicated chemical equilibria based on the weakly acidic character of MAP. MAP-12K aqueous solution behaves as if it is a binary mixed surfactant solution of hydrophobic dialkyl surfactant and hydrophilic monoalkyl surfactant in spite of a single component solution.

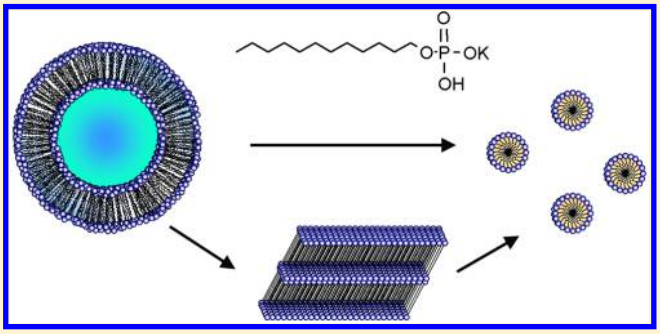

INTRODUCTION

Alkyl phosphates have been applied to emulsifiers, wetting agents, solubilizers, cleansers, and dispersing agents.[1] Although widely used alkyl phosphates were originally a mixture of mono- and dialkyl type,[2] the establishment of industrial preparation methods for high purity monoalkyl phosphate (MAP) has resulted in the novel application of this surfactant. Since MAP salts have been confirmed to be mild toward human skin, it has also been applied to skin-cleanser products.[3,4]

Although MAP has a long history as an industrial surfactant, there are only a few reports describing the basic aqueous solution properties of MAP. The cmc values of the aqueous solution of some MAP mono- or disalts have been determined by surface tension[5] and dynamic light scattering.[6] Then, Nakagaki et al. discussed the states of MAP disodium salts adsorbed at the air/water interface through the surface tension measurements.[7]

Imokawa et al. have described the highly strange water solubility of MAP salts, which does not follow the general solubility theory.[3] It means that, in a MAP salt aqueous solution, some precipitates appear from a certain dilute concentration and disappear again at a higher concentration. Then, Arakawa et al. have assumed that the characteristic water solubility might be caused by the formation of quaternary neutralized dimer, which consists of MAP monosalt and unneutralized MAP.[8]

From the viewpoint of aggregation behavior, the micelle size and the aggregation number of MAP disalts were studied.[6] Then, it has been mainly investigated that MAP salts can form vesicle aggregates in spite of the single alkyl chain surfactant, although vesicle aggregation has been thought to be one of the characteristics of double tailed surfactants. Ravoo et al. showed the vesicle formation properties of MAP salts which have branched alkyl chains and discussed the effect of pH on the vesicle size.[9] Pozzi et al. observed the spontaneous vesicle formation of monopolyprenyl phosphates.[10] Walde et al. studied the vesicle formation of unneutralized MAP in detail, and the most stable vesicle can be seen at the pK_a.[11] This vesicle formation has also been assumed to be based on the "quaternary neutralized dimers" because these dimers have the adequate double tailed structures to form vesicle aggregates.

On the other hand, the transition from vesicle to micelle has been a kind of interesting behavior because a more highly ordered structure like a vesicle spontaneously translates into a

Received: July 17, 2012
Revised: August 14, 2012
Published: August 17, 2012

dx.doi.org/10.1021/jp307070e | J. Phys. Chem. B 2012, 116, 11225−11233

less highly ordered structure like a micelle with an increase in surfactant concentration. Such an interesting phenomenon has been observed in some systems of surfactants and polymers. It has been often observed in single-tailed anionic and cationic surfactant mixed aqueous solutions.[12−14] These vesicles are formed by dimers consisting of anionic and cationic surfactants, which are combined strongly by the electrostatic interaction, and behave like double-tailed surfactants. Then, excess ionic surfactant in bulk starts forming micelles at higher concentration than the onset concentration of the vesicle formation. Recently, vesicle-to-micelle transition in single surfactant systems has also been reported. These surfactants are single-tailed ones which have a carboxylate headgroup.[15,16] Although the mechanism of this aggregation behavior has still not been determined, it has been assumed to result from double-tailed dimer formation between neutralized anionic species and unneutralized acidic ones due to hydrogen bonding. This dimer is really similar to the quaternary neutralized MAP dimer mentioned above. Then, a nonionic diblock copolymer also shows this interesting transition by controlling concentration and temperature.[17] From these examples, it is clear that vesicle-to-micelle transition should occur only when the appropriate condition, which includes concentration, composition, temperature, pH, and so on, can be held.

Although the characteristics like the strange water solubility and the vesicle formation of MAP salts have been found out, the continuous aggregation behavior including the vesicle and precipitate formation for MAP salts with increase in concentration of the aqueous solution has still not been clarified. Through this investigation, we have confirmed the vesicle-to-micelle transition also occurs in MAP aqueous solution. Moreover, since MAP is a kind of bivalent anionic surfactant, the degree of neutralization should affect seriously the aggregation behavior and the psychochemical properties of the solution. However, in the previous studies, it seems that this factor has been dealt with vaguely. Whereas various measurements have been performed under control of pH of aqueous solutions, the ion strengths in those systems should have been different from each other. Since MAP is a kind of weak acid salt, the aggregation behavior should have been highly affected by the ion strength in the system, which depends on the degree of neutralization, adding salt concentration, and amounts of acid/alkali used for pH control. Therefore, it is especially important to control the molar ratio of the counterion to MAP, which is called the molar degree of neutralization (D.N.), rather than the pH value.

In this study, we have totally investigated the solubility and the aggregation behavior including the precipitation, vesicle formation, and vesicle micelle transition of a MAP salt in water with increase in concentration using half neutralized MAP monopotassium salt (MAP-12K), whose D.N. value is constant 1.0.

EXPERIMENTAL SECTION

Materials. Monododecyl phosphate (MAP-12H, >99%), as shown in Figure 1, was supplied by Kao Corporation (Tokyo, Japan) and used without further purification. An 8 mol dm^{-3} KOH aqueous solution for quantitative analysis (Wako Pure Chemical Industries. Ltd., Osaka, Japan) and an oil-soluble dye, *o*-toluene-azo-*β*-naphthol (Wako Pure Chemical Industries. Ltd.), were used as received. Distilled water, with a surface tension of 72.4 mN m^{-1} at 25 °C was used to prepare the sample solutions. Monopotassium monododecyl phosphate, designated as MAP-12K (Figure 1), was prepared in solution by mixing of MAP-12H and a molar equivalent of KOH solution. After all sample solutions had been heated to 70 °C once, they were left to stand for 1 week at 25 °C to settle any precipitates prior to further measurements.

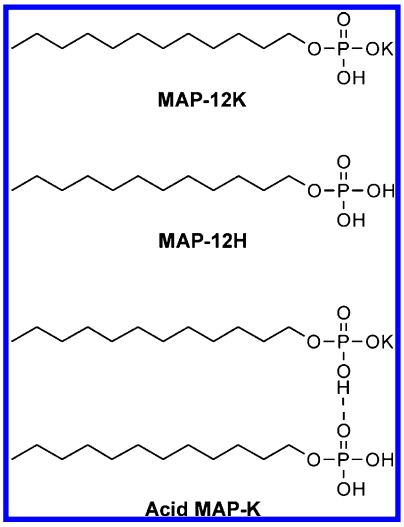

Figure 1. Structures of monoalkyl phosphate derivatives.

Equilibrium Surface Tension Measurements. The surface tension of the aqueous MAP-12K solutions was measured at 25 °C using the Wilhelmy Pt plate technique with K-100MK2 tensiometer (Krüss GmbH, Hamburg, Germany). For those test solutions containing precipitates, the measurements were performed after the precipitates had settled to the bottom of the vessels.

Elemental Analysis of Precipitate. The precipitate generated in 3.00 dm^3 of the test solution at 5.00 × 10^{-2} mol dm^{-3} was filtered and vacuum-dried in a desiccator for several days. The phosphorus and potassium contents in the sample were determined by wet-ashing (H_2SO_4−H_2O_2)/inductively coupled plasma atomic emission spectroscopy (ICP-AES; JY238, Jobin Yvon S.A.S., France) and by wet-ashing (H_2SO_4−H_2O_2)/atomic absorption spectrometry (AAS; Z-6100, Hitachi, Japan), respectively.

Quantitative Analysis of Solution Concentrations. Approximately 2 mL of the solution or clear supernatant of the samples including precipitate was sampled so as not to disturb any precipitate. 0.5 mL of 1 mol dm^{-3} HCl aqueous solution and 1.0 mL of 0.2 wt % hexadecanol in hexane were added to the sample solution as an internal standard. A 4 mL portion of diethylether was also added, and the test solutions were shaken vigorously. Then, 2 mL of the upper ether layer was sampled, and the solvent was evaporated after methylation using diazomethane. The sample residue was dissolved in 2 mL of hexane. The MAP-12H in the hexane solutions was quantitatively analyzed using gas chromatography (GC; Agilent 6850 series II) with a J&W Scientific Ultra 1 column (Agilent Technologies, Palo Alto, CA).

Measurement of Oil-Soluble Dye Solubilization. A 5 mL portion of test solution and the required amount of oil-soluble dye, *o*-toluene-azo-*β*-naphthol, were mixed in a 10 mL centrifuge tube using a vortex mixer. The tube was then gently shaken for a few days in a water bath at 25 °C, followed by filtering to remove the insoluble excess of dye, using a 5 mL syringe and a disposable filter unit DISMIC-13P (Tokyo Roshi Kaisha, Tokyo, Japan). A 4.00 mL portion of ethanol was added

to 1.00 mL of the filtrate, and the absorbance (ABS) of this solution was measured at 486 nm using a spectrophotometer (U-3300, Hitachi Corp., Tokyo, Japan) to determine the amount of solubilized dye.

Differential Scanning Calorimetry. Differential scanning calorimetry (DSC; DSC6100, SII Nano Technology Inc., Chiba, Japan) was performed using samples in sealed silver pans. Measurements of MAP-12K samples were performed at a scan rate of 0.5 °C min^{-1} in the temperature range 20−80 °C. Samples that contained precipitates at 25 °C were thoroughly stirred and then transferred into the sample pans.

Steady-State Fluorescence Measurements. Steady-state fluorescence measurements employing pyrene (1.0×10^{-6} mol dm^{-3}) as the probe were carried out using a spectrofluorometer (F-7000, Hitachi Corp., Tokyo, Japan). Emission spectra were recorded at an excitation wavelength of 339 nm. For the test solutions containing precipitates, only homogeneous supernatant solutions were used for measurements after settling of the precipitates at 25 °C for 1 week. After the test solution containing pyrene had been heated to approximately 70 °C, it was stirred at 25 °C for a few days and then measured.

Negatively Strained Transmission Electron Microscopy (TEM). An electron microscope, JEM2000 (JEOL Ltd., Tokyo, Japan), operating at a voltage of 80 kV was used for TEM measurement. A drop of 1.5×10^{-3} mol dm^{-3} of MAP-12K aqueous solution was placed on the carbon-coated copper grid and was allowed to stand for 2 min. The excess solution was blotted off with filter paper followed by staining with 2% aqueous uranyl acetate solution.

Cryo-Scanning Electron Microscopy (SEM). A drop of MAP-12K aqueous solution was applied to the grid and was rapidly frozen with liquid-nitrogen. An electron microscope, S-4000 (Hitachi Corp., Tokyo, Japan) equipped with cryo-chamber, operating at a voltage of 7.5 kV was used for SEM measurement. After a specimen was etched at a temperature range from −150 to −90 °C and coated with gold, the observation was performed at −120 °C.

RESULTS

Equilibrium Surface Tension. Figure 2 shows the equilibrium surface tension (γ) against log C (where C is the total concentration) for MAP-12K in water at 25 °C in the concentration range from 1.0×10^{-4} to 1.0 mol dm^{-3}. We can see a complicated curve with three break points, which is different from a typical surface tension curve, which has only one break point at the critical micelle concentration (cmc), for conventional surfactants such as sodium dodecyl sulfate (SDS). The concentrations of these break points are designated as C_1 (=1.2×10^{-3} mol dm^{-3}), C_2 (=4.0×10^{-3} mol dm^{-3}), and C_3 (=2.0×10^{-2} mol dm^{-3}) from lower to higher concentration. Below C_1, γ decreases linearly with an increase in concentration. However, interestingly, a small plateau appears at C_1 and the γ values between C_1 and C_2 nonlinearly decrease again. This is a highly unique characteristic because γ vs log C plots in dilute solutions generally decrease linearly without a break point.

Through the concentration range from C_2 to C_3, γ is almost constant at 23 mN m^{-1}. At C_3, γ increases gradually again until a constant value is achieved at approximately 27.5 mN m^{-1}, which is very low compared with conventional anionic surfactants (e.g., SDS: 40 mN m^{-1})[18] and is almost the same as that for hydrocarbons such as n-octane.[19] This indicates that MAP-12K is very hydrophobic for an anionic surfactant. A few similar γ−log C curves that have a few break points have been

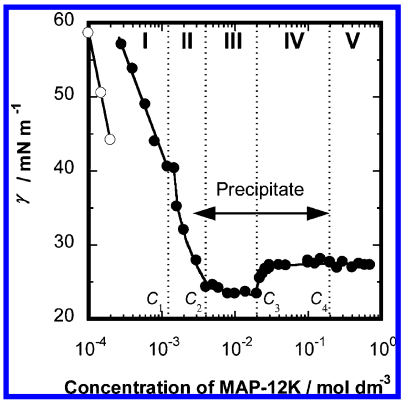

Figure 2. Equilibrium surface tension (γ) versus log C for MAP-12K (●) and Acid MAP-K (○) aqueous solution at 25 °C. C_1, C_2, and C_3 indicate the break point concentrations. C_4 indicates the concentration where the precipitates disappear. Regions I, II, III, IV, and V show the concentration regions: (I) below C_1 where solution is transparent and γ decreases linearly, (II) between C_1 and C_2 where partially precipitate exists and γ decreases nonlinearly, (III) between C_2 and C_3 where precipitate exists and γ shows plateau, (IV) between C_3 and C_4 where precipitate exists and γ increases, and (V) above C where solution is transparent.

reported. Meguro et al. investigated a mixed surfactant aqueous solution containing SDS and polyoxyethylene-*n*-alkylether having a variety of polyoxyethylene chain lengths,[20−23] and reported a γ curve with almost the same shape as that in Figure 2 for an aqueous solution of SDS containing a certain small amount of nonionic surfactant. Villeneuve et al. also reported a similar γ curve for a mixed surfactant aqueous solution of SDS and decyltrimethylammonium bromide.[24] From thermodynamic analysis, they proposed that the break points were the critical vesicle concentration (cvc) and the cmc. However, Figure 2 basically differs from these examples, in that it was measured for a solely MAP-12K system. The three break points in Figure 2 should reflect some aggregation behavior of MAP-12K itself with increasing concentration. These characteristics about the γ vs log C plots are thought to result from some aggregate formation. It will be discussed in detail in the Discussion section.

Analysis of Precipitates. Another interesting phenomenon, which may also result from characteristic aggregation, is that the precipitate is observed only within a certain concentration range of MAP-12K, over approximately 2 orders of magnitude, as shown in Figure 2. This characteristic for MAP-12 Na salt has also been reported by Imokawa et al.[3] However, it has not been confirmed what the precipitate is. The generation of precipitate deposition starts to be visually observed at 2.7×10^{-3} mol dm^{-3} less than C_2, and the amount of precipitate increases with an increase in the total MAP-12K concentration below C_3. However, in the higher concentration region than C_3, the amount of precipitate decreases with increasing concentration of MAP-12K and disappears at C_4 (ca. 2.00×10^{-1} mol dm^{-3}). The precipitate deposited at 5.00×10^{-2} mol dm^{-3} between C_3 and C_4 was identified by elemental analysis.

Table 1 shows the contents of MAP-12H and the degree of neutralization (D.N.) in the precipitate and the aqueous phase, which were calculated from the elemental analysis results. The D.N. values show the molar equivalent of potassium to MAP in each phase, which were determined by the molar ratio of potassium to phosphorus content (=K/P). These results reveal that ca. 12 mol % of total MAP is precipitated from the solution

dx.doi.org/10.1021/jp307070e | J. Phys. Chem. B 2012, 116, 11225−11233

Table 1. Elemental Analysis for the Contents of MAP and Potassium in the Precipitate and Bulk Phase

Analysis Data for Precipitate[a]	
phosphorus (wt %)	11
potassium (wt %)	7.0
total precipitate (g)	1.6204
Precipitated Components[b]	
monododecyl phosphate (mol)	5.8×10^{-3}
potassium (mol)	2.9×10^{-3}
D.N.	0.50
Components in Aqueous Phase[b]	
monododecyl phosphate (mol)	4.7×10^{-2}
potassium (mol)	4.4×10^{-3}
D.N.	1.1

[a]25 °C, 1.00 dm^3 of 5.00×10^{-2} mol dm^{-3} aqueous solution for MAP-12K. [b]All data were calculated from the elemental analysis results for the precipitates.

and the D.N. value of the precipitate is 0.5 which means that the precipitate is quaternary neutralized MAP-12H. This implies that the precipitate is a bimolecular aggregate composed of MAP-12H and MAP-12K. The formation of this water-insoluble dimer aggregate has been presumed from the results of alkaline titration for MAP-12H solution,[8] and from conductivity measurements for monopotassium hexadecyl phosphate aqueous solution.[25] In this study, this hypothesis is directly confirmed by analysis of the precipitate generated spontaneously in the MAP-12K aqueous solution. Such a dimer aggregate, which consists of unneutralized and neutralized acidic surfactants, is known to be also formed in a fatty acid soap aqueous solution, and is referred to as "acid soap".[26] Therefore, the dimer aggregate obtained from MAP-12K aqueous solutions was named "Acid MAP-K" and the structure is shown in Figure 1.

The γ for Acid MAP-K aqueous solution at 25 °C is also plotted by open dots in Figure 2. The abscissa is indicated by the MAP concentration, which is equal to twice the Acid MAP-K concentration. The γ plots decrease linearly with an increase in concentration. However, Acid MAP-K reaches its solubility limit at around 2.00×10^{-4} mol dm^{-3} and a large amount of precipitate is observed in the concentration region greater than 2.00×10^{-4} mol dm^{-3}. Therefore, the onset concentration of the Acid MAP-K precipitation in MAP-12K aqueous solution is much greater than the actual solubility limit of Acid MAP-K itself. It clearly suggests that MAP-12K solution does not consist of Acid MAP-K only.

Determination of Actual MAP Concentrations in Each Phase. In order to determine the changes in the amount of Acid MAP-K precipitates and MAP molecules dissolved in the bulk phase with the change in the total concentration of MAP-12K, MAP-12K aqueous solutions of various concentrations were quantitatively analyzed using gas chromatography. The quantities of the precipitates were calculated from the differences between the total MAP concentration and that in the homogeneous aqueous phase as follows:

$$C_{pre} = C_{total} - C_{sol} \quad (1)$$

where C_{pre}, C_{total}, and C_{sol} show the molar concentrations of MAP molecules in the precipitates, in the total system, and in the water phase, respectively. The total potassium concentration is equal to C_{total}, and Acid MAP-K has a D.N. value of 0.5. The D.N. value of MAP in the aqueous phase, DN_{sol}, is determined by eq 2:

$$DN_{sol} = (C_{total} - 0.5C_{pre})/C_{sol} \quad (2)$$

Figure 3 shows the molar concentrations of MAP molecules in the aqueous phase and the Acid MAP-K precipitates,

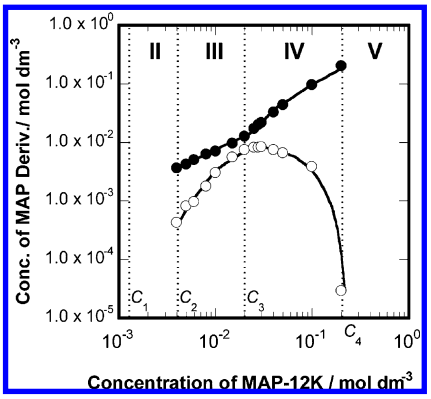

Figure 3. MAP molecule concentrations in the bulk phase (●) and the solid phase (precipitate) (○) at 25 °C: C_1, C_2, C_3, and C_4 are indicated in Figure 2. Regions II–V are also as indicated in Figure 2.

respectively. Both of the MAP-12H concentrations in the aqueous phase and in the precipitate phase increase in the concentration region between C_2 and C_3. Then, the concentration of the precipitated MAP has a maximum at C_3 followed by starting a decrease again, while that in the water phase continues to increase above C_3.

Figure 4 shows the D.N. value of MAP-12H in the aqueous phase against the total MAP concentration. The D.N. value in

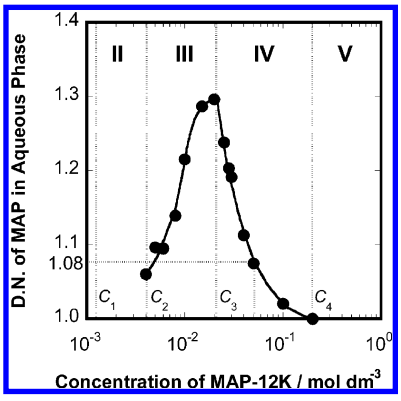

Figure 4. Degree of neutralization (D.N.) for MAP in the bulk phase. C_1, C_2, C_3, and C_4 are indicated in Figure 2. Regions II–V are also as indicated in Figure 2.

the aqueous phase shows a rapid increase toward C_3 and reaches a maximum of 1.3 at C_3 followed by rapid decrease to 1.0 above C_3 with the disappearance of the precipitates. According to the elemental analysis, the D.N. value in the aqueous phase for the 5.00×10^{-2} mol dm^{-3} solution is estimated to be 1.1, as shown in Table 1. Figure 4 shows that the D.N. value for the 5.00×10^{-2} mol dm^{-3} solution is 1.08, which agrees well with the elemental analysis results. In this concentration region, where precipitation occurs, the D.N. value for the bulk phase varies greatly from 1.0 to 1.3, which suggests that the composition of the bulk phase, which consists

dx.doi.org/10.1021/jp307070e | J. Phys. Chem. B 2012, 116, 11225–11233

of monoanion type, dianion type, and MAP-12H, might also gradually change with the total concentration of MAP-12K.

Usually, C_2 might be regarded as the solubility limit of Acid MAP-K. Therefore, considering the solubility theory, the amount of the precipitates should increase proportionally with increase in total concentration, while the concentration of the bulk phase remains constant. However, we can see in Figure 3 that both Acid MAP-K and dissolved MAP increase above C_2. Moreover, unexpected as it is from the solubility theory, the amount of precipitates decreases above C_3. These characteristic phenomena are also assumed to be caused by the composition change of MAP derivatives due to the complicated aggregation behavior based on the chemical equilibrium of the MAP system. Concerning the complicated aggregation behavior, we will investigate in detail below.

Solubilization of Oil-Soluble Dye. Since the γ plots for MAP-12K have three break points (Figure 2), the solubilization of an oil-soluble dye, *o*-toluene-azo-*β*-naphthol, in MAP-12K aqueous solutions was investigated to determine the cmc. The ABS of the solubilized dye at 486 nm was observed at 25 °C, and the results are shown in Figure 5. The ABS starts to

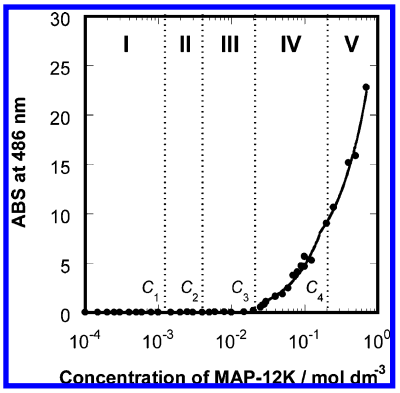

Figure 5. Solubilization ability of the MAP-12K aqueous solution for *o*-toluene-azo-*β*-naphthol at 25 °C. ABS indicates the absorbance of the dye at 486 nm. C_1, C_2, C_3, and C_4 are indicated in Figure 2. Regions I–V are also as indicated in Figure 2.

increase abruptly at C_3, which suggests that the micelles, which have a hydrophobic core with sufficient size to solubilize dye molecules, begin to be formed at C_3. In addition, this result also suggests that the aggregation of Acid MAP-K precedes micelle formation.

DSC Measurements. DSC traces for MAP-12K aqueous solutions are shown in Figure 6. 4.00×10^{-1} mol dm^{-3} of the MAP-12K aqueous solution is a transparent micellar solution. The DSC trace for this solution (line 5) exhibits a single endothermic peak at 17 °C, which absolutely indicates the Krafft point of MAP-12K. In the concentration region between C_3 and C_4, both of the precipitates of Acid MAP-K and the solubilization of oil-soluble dye can be observed. That is, the micelles and precipitates interestingly coexist at this concentration. In the DSC trace (line 4) for the 1.00×10^{-1} mol dm^{-3} MAP-12K aqueous solution, two clear endothermic peaks at 17 °C and a minute peak at 53 °C are observed. The peak at 17 °C can be determined to be the Krafft point of the MAP-12K, because it can also be seen in line 5. Another peak at 53 °C might be the Krafft point of Acid MAP-K because it coincides with the DSC peak of the Acid MAP-K alone aqueous dispersion (line 6). As the total MAP concentration becomes more dilute, the peak at 17 °C relatively becomes smaller and

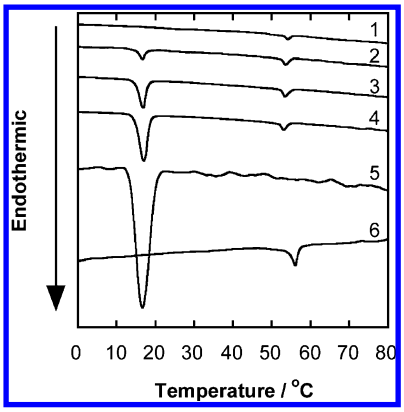

Figure 6. DSC traces for MAP-12K aqueous solutions and Acid MAP-K aqueous dispersion. (1) 1.5×10^{-2} mol dm^{-3}, (2) 5.0×10^{-2} mol dm^{-3}, (3) 7.0×10^{-2} mol dm^{-3}, (4) 1.0×10^{-1} mol dm^{-3}, and (5) 4.0×10^{-1} mol dm^{-3} of MAP-12K aqueous solutions; (6) 5.0×10^{-2} mol dm^{-3} of Acid MAP-K aqueous dispersion.

another peak at 53 °C becomes larger. Then, at 5.00×10^{-2} mol dm^{-3}, the intensity of these two peaks becomes almost equal (line 2). Finally, at 1.50×10^{-2} mol dm^{-3}, which is slightly lower than the cmc, only a small endothermic peak can be confirmed at 53 °C (line 1). In the concentration region, less than 1.50×10^{-2} mol dm^{-3}, the test solutions are so dilute that DSC peaks were not detected at all. These DSC measurements provide clear evidence that the Acid MAP-K are generated only in a certain dilute concentration range around the cmc in the MAP-12K aqueous solution. Moreover, it was also clarified that, despite the single component solution of MAP-12K, it includes two chemical species, MAP-12H potassium salts and Acid MAP-K.

Steady-State Fluorescence Measurements. The characteristic emission spectrum of pyrene monomer in the visible region shows five maxima at 370–400 nm. The intensity ratio for the first and third peaks of the pyrene emission spectrum, I_1/I_3, is well-known to indicate the polarity of the probe environment, and a decrease of I_1/I_3 denotes a decrease in the polarity.[27] In dilute surfactant aqueous solutions below the cmc, I_1/I_3 is commonly around 1.7–1.8, which agrees with the value of the saturated pyrene aqueous solution. When pyrene molecules are solubilized in the hydrophobic core of micelles above the cmc, I_1/I_3 falls abruptly at the cmc and maintains a low constant value above the cmc. Therefore, this method is often used to determine the cmc of surfactant solutions or confirm the presence of surfactant aggregates which have a hydrophobic core. Plots of I_1/I_3 vs log C for MAP-12K aqueous solutions at 25 °C are shown in Figure 7. The value of I_1/I_3 remains constant at ca. 1.7 for lower concentrations below C_1, which is almost the same value as that in water. The onset of a decrease in I_1/I_3 occurs at C_1, with a gradual decrease until the MAP-12K concentration reaches C_3 (I_1/I_3 ca. 1.1). A plateau in the I_1/I_3 vs log C plot appears again beyond C_3 (=cmc), which suggests that all of the pyrene molecules in the system are solubilized in the micelle core. The most interesting feature of these plots is the gradual decrease in I_1/I_3 between C_1 and C_3. This is unlike the behavior observed for typical surfactant solutions such as SDS, in which a sharp drop of I_1/I_3 is observed at the cmc. These measurements were performed using the supernatant without precipitates, so that the I_1/I_3 values should not be affected by precipitation. This decrease might indicate that some kind of aggregate, which has a

dx.doi.org/10.1021/jp307070e | J. Phys. Chem. B 2012, 116, 11225–11233

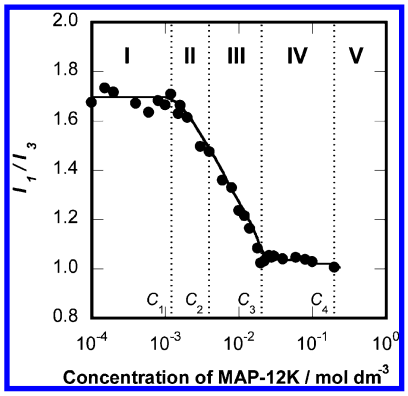

Figure 7. I_1/I_3 versus log C for MAP-12K in aqueous solution with pyrene at 25 °C. Experiments were performed using only homogeneous supernatants of the test solutions in the concentration range where precipitation occurred. C_1, C_2, C_3, and C_4 are indicated in Figure 2. Regions I–V are also as indicated in Figure 2.

hydrophobic core to solubilize pyrene molecules, is present in the bulk phase between C_1 and C_3 below the cmc.[28]

Recently, it has been reported that a broad emission spectrum of pyrene can be observed in only dilute surfactant solution including some aggregate, which is called pre-micelle, below the cmc.[28,29] The appearance of this band is attributed to the formation of an excited state dimer (excimer) which is formed by the reaction of an excited pyrene molecule with another one in the ground state.[30] The excimer can be formed only at concentrations higher than 1 μM or when it is dissolved in hydrophobic microdomains. In Figure 8, the excimer

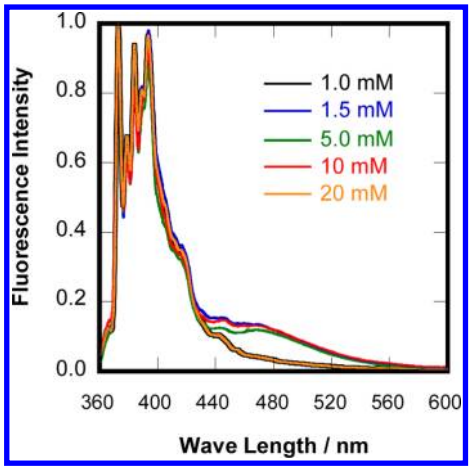

Figure 8. Emission spectra of pyrene (1.0×10^{-6} mol dm^{-3}) in MAP-12K aqueous solutions at 25 °C. DSC traces for MAP-12K aqueous solutions and Acid MAP-K aqueous dispersion. All intensity was normalized by that of the strongest first peak (373 nm) of pyrene monomer. The spectra for 1.0×10^{-3} and 2.0×10^{-2} mol dm^{-3} completely coincided. Excimer peaks around 470 nm were observed at 1.5×10^{-3}, 5.0×10^{-3}, and 1.0×10^{-2} mol dm^{-3}.

emission band with a maximum around 470 nm can be seen at only a certain concentration range between C_1 and C_3 (1.5×10^{-3}, 5.0×10^{-3}, and 1.0×10^{-2} mol dm^{-3}) while it is not observed at 1.0×10^{-3} mol dm^{-3} below C_1 and 2.0×10^{-2} mol dm^{-3} (C_3 = cmc). These results should also suggest that some aggregate, which is generally called "pre-micelle", exists during a wide concentration range from C_1 to C_3.

Negatively Stained TEM and Cryo-SEM Observation. It is quite interesting that some aggregates exist in the concentration range between C_1 and C_3 below the cmc as mentioned above. TEM observation was performed at 1.5×10^{-3} mol dm^{-3} to determine the morphology of the pre-micelle (Figure 9A). Then, we can see about 200 nm of unilamellar

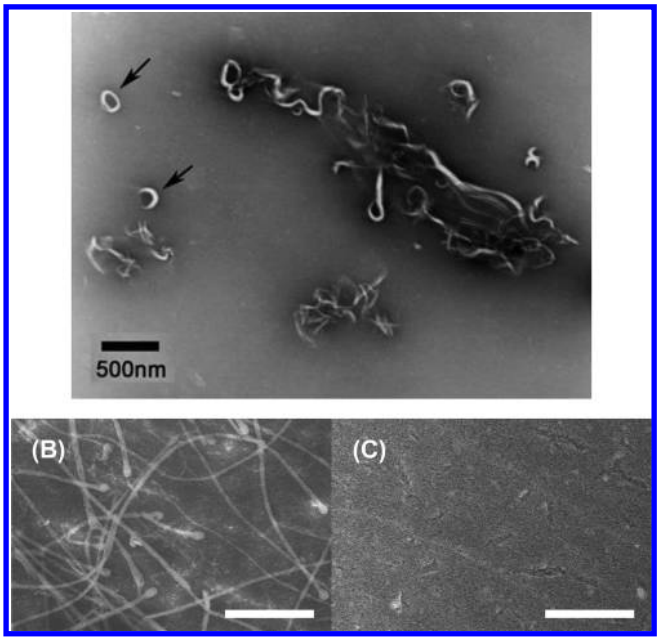

Figure 9. Electron micrographs for MAP-12K aqueous solution. (A) Negatively strained transmission electron micrograph for 1.5×10^{-3} mol dm^{-3} aqueous solution. Arrows show unilamellar vesicles. (B and C) Cryo-scanning electron micrographs for 1.5×10^{-3} and 4.0×10^{-1} mol dm^{-3} aqueous solutions, respectively. The white scale bar is 3.00 μm.

vesicles and quite giant entangled tubular vesicle aggregates. These vesicle aggregates in the bulk phase could cause the solubilization of pyrene. Whereas sphere vesicle formation of MAP or its salts in the higher concentration region has been reported,[9–11] the vesicle formation in the dilute solution and the tubular vesicle formation have not been observed until now. Much more interestingly, these vesicles have various shapes. At this concentration, the solution is clear without precipitates and these aggregates seem to be formed spontaneously. However, the various shapes should suggest that they are not thermodynamically stable. Therefore, the same sample was also observed by cryo-SEM because a possibility that negative staining treatment affected the aggregation state could not be resolved about the TEM image (Figure 9B). We can also confirm a lot of quite long tubular vesicles that have spherical vesicles at the ends exist.

Moreover, cryo-SEM observation was also performed at 4.0×10^{-1} mol dm^{-3} above the cmc (Figure 9C). The aggregates with highly ordered structure cannot be confirmed at this high concentration at all. It suggests that MAP-12K aqueous solution might form a small micelle above the cmc, that is, vesicle-to-micelle transition. The aggregation number of MAP-12 monosalt micelle has been reported to be as large as that of SDS micelle by SLS measurements.[6] The micellar size of MAP-12K might be about 5 nm because the molecular size of MAP-12K is close to that of SDS. Therefore, the micelles of MAP might be too small to be observed by SEM. We'd like to deal

dx.doi.org/10.1021/jp307070e | J. Phys. Chem. B 2012, 116, 11225–11233

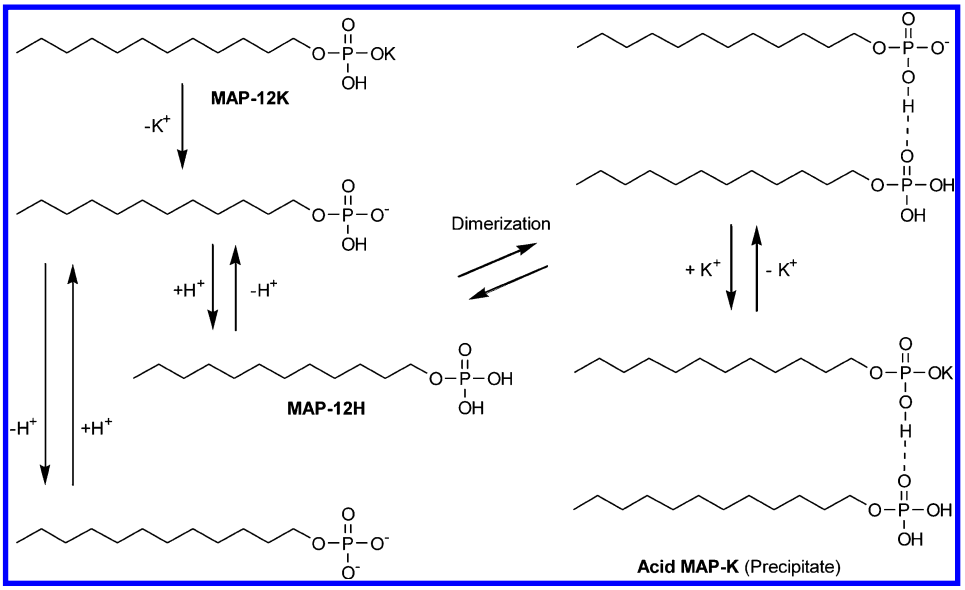

Figure 10. Chemical equilibrium model for MAP-12K in dilute aqueous solution.

with the vesicle formation and vesicle-to-micelle transition in the Discussion section again.

DISCUSSION

From the results of this study, a lot of characteristics can be seen for the MAP-12K aqueous solution at 25 °C. In this section, we will totally discuss how MAP-12K molecules exist in water and what aggregation behavior they show with increase in total MAP-12K concentration. Regions I–V used here are based on the concentration regions shown in Figure 2.

Region I. ($C < C_1$) In the quite dilute concentration region below C_1, the solution is a transparent solution. The γ plots vs log C also decrease linearly like conventional surfactant solutions. The solubilization of pyrene and oil-soluble dye cannot be observed at all here. Therefore, it is assumed to be monomeric MAP-12K solution. The area per molecule, which was calculated by the Gibbs adsorption equation, is 69.3 Å^2, which is almost equal to that of a conventional anionic surfactant, sodium polyoxyethylene(2) dodecylether sulfate.[18]

Region II. ($C_1 \leq C < C_2$) A small plateau appears on the γ plots at C_1, and the γ values nonlinearly decrease with an increase in total concentration. We can see three characteristics which are different from general γ vs log C plots. (1) The rereduction of γ after reaching the plateau at C_1: Generally, the γ value should not decrease steeply after it reaches the plateau once because the plateau on γ plots means a kind of phase separation for surfactant. (2) The nonlinear decrease: If the adsorption of MAP salt to the air/water interface follows Gibbs' monolayer model, γ plots should be linear. (3) The deposition of precipitates of Acid MAP-K at slightly lower concentration than C_2: Since precipitation is clearly a kind of phase separation, γ plots should generally show a plateau at the concentration where precipitation starts. In order to explain these three characteristics, it is thought to be the most rational that some aggregation occurs at C_1 and the composition of MAP derivatives in this system gradually changes with an increase in concentration.

The small plateau appearance at C_1 is thought to reveal the onset of aggregation for MAP-12K. The existence of some aggregate is suggested by Figures 7 and 8, which shows the existence of an environment where pyrene can be restricted and the excimer of pyrene can be formed in water. Such an aggregate is evidently unilamellar vesicle or giant tubular vesicle that we can visually confirm in the TEM and SEM images (Figure 9A,B). Then, these vesicle aggregates are assumed to be made of Acid MAP-K because Acid MAP-K starts depositing at slightly higher concentration. Although Acid MAP-K is already formed, the amount is so small that it might be able to exist in the bulk phase due to the vesicle formation. Then, the precipitates of Acid MAP-K might deposit from the bulk when its amount reaches a certain solubility limit concentration around C_2. Besides, Acid MAP-K is sure to be spontaneously formed in the complicated chemical equilibrium system of MAP-12K in water (Figure 10).

The nonlinear decrease of γ plots suggests the surfactant composition of monolayer at the air/water interface or of bulk phase changes. As mentioned in Figure 10, MAP-12K might cause successive changes in the composition of the chemical species with the change of total concentration of MAP-12K. Especially, the generation of much more hydrophobic Acid MAP-K should give a strong effect on the compositions and the properties of monolayer and bulk. Therefore, the γ plots in this region are assumed to decrease nonlinearly with an increase in concentration.

Region III. ($C_2 \leq C < C_3$) The γ plots reach a minimum value (=27.5 mN m^{-1}) which is maintained until C_3. This minimum γ value is very low for an anionic surfactant. Since hydrophobic Acid MAP-K should dominate all of the system below the cmc, Acid MAP-K should preferentially adsorb to the air/water interface. Then, the monolayer on the surface reaches saturation at C_2, resulting in the very low γ value.

On the other hand, as mentioned in the Results section, both amounts of precipitated Acid MAP-K and dissolved MAP derivatives increase even above C_2. Further, vesicles are assumed to be in this region due to the exicmer emission spectra of pyrene (Figure 8). It suggests that the composition of MAP derivatives keeps changing gradually in the chemical equilibrium of Figure 10 with an increase in total concentration. The increase in the D.N. value of the bulk phase in Figure 4 also reveals the continuous composition change.

Region IV. ($C_3 \leq C < C_4$) C_3 is the cmc of MAP-12K aqueous solution. It can be confirmed by the solubilization of

dx.doi.org/10.1021/jp307070e | J. Phys. Chem. B 2012, 116, 11225–11233

oil-soluble dye measurement (Figure 5) and the final value of I_1/I_3 which gives a very hydrophobic environment like micelle core (Figure 7). In addition, vesicles also might disappear in this region because the excimer peak of pyrene in Figure 8 became unable to be detected suddenly above the cmc. The disappearance of vesicles can also be confirmed by the SEM image (Figure 9C). When the micellization of monomeric MAP derivatives proceeds, the chemical equilibria in Figure 10 should move to the direction where Acid MAP-K generation is prohibited. Consequently, whereas the amount of Acid MAP-K precipitate reaches the maximum at C_3 and subsequently decreases with an increase in concentration, coexisting dissolved MAP derivatives continue to increase (Figure 3). Then, Acid MAP-K precipitate disappears at C_4. The DSC traces in Figure 6 evidently back up the successive composition change.

Region V. ($C_4 \leq C$) In this region, the solution is a homogeneous micellar solution whose Krafft point is 17 °C. It can be confirmed by DSC measurement (Figure 6, line 5) and SEM observation (Figure 9C).

Pseudobinary Mixed Surfactant Solution of MAP-12K. MAP-12K in water generates both hydrophilic monomeric MAP derivatives and very hydrophobic Acid MAP-K in the chemical equilibrium system due to its weakly acidic character. Because the hydrophilic/hydrophobic characters of these species are significantly different from each other, they seem to behave as a mixed surfactant system including a hydrophilic surfactant and a hydrophobic one in spite of the single component system of MAP-12K. While the hydrophobic Acid MAP-K forms vesicle aggregates at very dilute concentration, C_1, the excess Acid MAP-K deposits at higher concentration between C_2 and C_4. Besides, the amount of monomeric hydrophilic MAP derivatives is increasing with an increase in total concentration, too, so that the concentration of them reaches its solubility limit at a certain concentration. This concentration is the cmc of MAP-12K, C_3. Such complicated aggregation behavior of MAP-12K in water is believed to cause the characteristics like the break points on γ plots and the deposition/disappearance of precipitates. The most different point of this "pseudo-binary mixed surfactant system" from real binary mixed surfactant systems is that each surfactant's composition successively changes with an increase in total concentration.

Also, in acylated phenylalanine salt aqueous solution, the similar phenomena like vesicle formation in dilute concentration and uncommon shape of γ plots have been observed. These have also been assumed to be caused by the half neutralized dimer formation.[16]

Vesicle Formation, Vesicle-to-Micelle Transition. Vesicle aggregates in Figure 9A and B clearly exist in transparent dilute solution of 1.50×10^{-3} mol dm^{-3} below C_2. They have varied shapes like unilamellar and very long tubular vesicles. This vesicle formation proceeds micellization; that is, it means vesicle-to-micelle transition occurs at C_3. Evidently, disappearance of vesicles can be seen in Figure 9C. It is also interesting that a more highly ordered structure such as a vesicle is transformed into a less highly ordered structure such as a micelle with increasing concentration. This characteristic transition can also be thought to result from the pseudobinary mixed surfactant solution.

Although these vesicles seem to form spontaneously, we doubt if they are thermodynamically stable because of their divided shapes and sizes. As Walde et al. have suggested that stable vesicles of MAP-12H are only formed in acidic condition around the pK_a (=1.8),[11] these vesicles may not also be thermodynamically stable. Especially, it seems that these giant tubular vesicles deposit easily as precipitates. However, this clear solution was stable for a few months without precipitation. Therefore, it has to be further discussed whether these aggregates spontaneously form or not.

CONCLUSION

Alkyl phosphate salts have been applied to a lot of industrial applications for a long time. However, the properties of aqueous solution have not been clarified except for some uncommon characteristics like the vesicle formation and the precipitate deposition only within a certain dilute concentration range. Therefore, in this study, the aggregation behavior of monopotassium monododecyl phosphate (MAP-12K) in aqueous solution with an increase in concentration was investigated in detail. MAP-12K produced a large amount of precipitate of a highly hydrophobic dimeric complex (Acid MAP-K) composed of unneutralized monododecyl phosphate and monopotassium salt only in a certain dilute concentration region. Vesicle aggregates have already been in much more dilute clear solution than that including precipitates. At the cmc, coexisting dissolved MAP-12 derivatives start forming micelles with vesicle-to-micelle transition. Furthermore, the hydrophobic Acid MAP-K precipitate disappears at 10 times higher than the cmc and the system finally becomes a clear homogeneous micellar solution. All these characteristics are thought to be based on the generation of Acid MAP-K, which is much more hydrophobic than dissolved MAP-12 derivatives, in the chemical equilibrium. Consequently, MAP-12K aqueous solution behaves as a pseudobinary mixed surfactant solution which consists of hydrophobic dialkyl surfactant and hydrophilic monoalkyl surfactant.

AUTHOR INFORMATION

Corresponding Author

*E-mail: sakai.takaya@kao.co.jp. Phone: +81-73-426-5065. Fax: +81-73-426-5067.

Notes

The authors declare no competing financial interest.

ACKNOWLEDGMENTS

We are grateful to Dr. Akira Kawamata and Mr. Isao Umemoto and Dr. Youhei Kaneko of Kao Corporation for providing the opportunity to perform this study and permission to publish this paper, to Dr. Kaoru Tsujii of Hokkaido University and Dr. Hideki Matsuoka of Kyoto University for enlightening discussions, and also to Ms. Yoriko Tamura for experimental assistance.

REFERENCES

(1) Jungermann, E.; Silberman, E. C. *Anionic Surfactants Part II*; Marcell Dekker: New York, 1976; p 495.
(2) Brown, A. D.; Malkin, T.; Maliphant, G. K. *J. Chem. Soc.* **1955**, 1584−1588.
(3) Imokawa, G.; Tsutsumi, H.; Kurosaki, T. *J. Am. Oil Chem. Soc.* **1978**, *55*, 839−842.
(4) Thau, P. *Surfactants in Cosmetic*, 2nd ed.; Marcel Dekker: New York, 1997; p 297.
(5) Cooper, R. S. *J. Am. Oil Chem. Soc.* **1963**, *40*, 642−645.
(6) Tahara, T.; Satake, I.; Matuura, R. *Bull. Chem. Soc. Jpn.* **1969**, *42*, 1201−1205.

(7) Nakagaki, M.; Handa, T. *Bull. Chem. Soc. Jpn.* **1975**, *48*, 630−635.
(8) Arakawa, J.; Pethica, B. A. *J. Colloid Interface Sci.* **1980**, *75*, 441−450.
(9) Ravoo, B. J.; Engberts, J. B. F. N. *Langmuir* **1994**, *10*, 1735−1740.
(10) Pozzi, G.; Birault, V.; Werner, B.; Dannenmuller, O.; Nakatani, Y.; Ourisson, G.; Terakawa, S. *Angew. Chem., Int. Ed. Engl.* **1996**, *35*, 177−180.
(11) Walde, P.; Wessicken, M.; Rädler, U.; Berclaz, N.; Conde-Frieboes, K.; Luisi, P. L. *J. Phys. Chem. B* **1997**, *101*, 7390−7397.
(12) Kaler, E.; W.; Herrington, K. L.; Iampietro, D. J.; Coldren, B. A.; Jung, H.; Zasadzinski, J. A. *Mixed Surfactant Systems*, 2nd ed.; Marcel Dekker: New York, 2005; p 289.
(13) Yin, H.; Huang, J.; Lin, Y.; Zhang, Y.; Qiu, S.; Ye, J. *J. Phys. Chem. B* **2005**, *109*, 4104−4110.
(14) Tsuchiya, K.; Nakanishi, H.; Sakai, H.; Abe, M. *Langmuir* **2004**, *20*, 2117−2122.
(15) Roy, S.; Dey, J. *Langmuir* **2003**, *19*, 9625−9629.
(16) Ohta, A.; Danev, R.; Nagayama, K.; Mita, T.; Asakawa, T.; Miyagishi, S. *Langmuir* **2006**, *22*, 8472−8477.
(17) Kim, S. Y.; Lee, K. E.; Han, S. S.; Jeong, B. *J. Phys. Chem. B* **2008**, *112*, 7420−7423.
(18) Dahanayake, M.; Cohen, A. W.; Rosen, M. J. *J. Phys. Chem.* **1986**, *90*, 2413−2418.
(19) Hiemenz, P. C.; Rajagopalan, R. *Principles of Colloid and Surface Chemistry*, 3rd ed.; Marcel Dekker: New York, 1997; p 257.
(20) Akasu, H.; Ueno, M.; Meguro, K. *J. Am. Oil Chem. Soc.* **1974**, *51*, 519−521.
(21) Takasawa, Y.; Ueno, M.; Meguro, K. *J. Colloid Interface Sci.* **1980**, *78*, 207−211.
(22) Takasawa, Y.; Ueno, M.; Sawamura, T.; Meguro, K. *J. Colloid Interface Sci.* **1981**, *84*, 196−201.
(23) Meguro, K.; Kanbe, T.; Esumi, K. *J. Am. Oil Chem. Soc.* **1983**, *60*, 1050−1052.
(24) Villeneuve, M.; Kaneshina, S.; Imae, T.; Aratono, M. *Langmuir* **1999**, *15*, 2029−2036.
(25) Suzuki, T.; Takei, H. *Nippon Kagaku Kaishi* **1986**, 633−640.
(26) Eagland, D.; Franks, F. *Trans. Faraday Soc.* **1965**, *61*, 2468−2477.
(27) Kalyanasundaram, K.; Thomas, J. K. *J. Am. Chem. Soc.* **1977**, *99*, 2039−2044.
(28) Sakai, T.; Kaneko, Y.; Tsujii, K. *Langmuir* **2006**, *22*, 2039−2044.
(29) You, Y.; Jiang, R.; Cao. *J. Colloid Polym. Sci.* **2009**, *287*, 839−846.
(30) Sivakumar, A.; Somasundaran, P. *Langmuir* **1994**, *10*, 131−134.